Journal of Materials Chemistry A

Accepted Manuscript

ROYAL SOCIETY OF CHEMISTRY

www.rsc.org/materialsA

Journal of Materials Chemistry A RSCPublishing

ARTICLE

Novel Z-Scheme Visible-Light-Driven Ag_3PO_4/Ag/SiC photocatalysts with Enhanced Photocatalytic Activity

Cite this: DOI: 10.1039/xoxxoooooox

Received ooth January 2012,
Accepted ooth January 2012

DOI: 10.1039/xoxxoooooox

www.rsc.org/

Zhihong Cheng, Fan Bing, Qiong Liu, Zhengguo Zhang and Xiaoming Fang*

Visible-light-driven Ag_3PO_4/Ag/SiC photocatalysts with different weight fractions of SiC were synthesized via an in-situ precipitation method and characterized by X-ray diffraction (XRD) and UV–vis diffuse reflectance spectroscopy (DRS). Under visible light irradiation (> 420 nm), the Ag_3PO_4/Ag/SiC photocatalysts degraded methyl orange and phenol efficiently and displayed much higher photocatalytic activity than that of pure Ag_3PO_4/Ag or SiC/Ag, and the Ag_3PO_4/Ag/SiC hybrid photocatalyst with 10% of SiC exhibited the highest photocatalytic activity. The quenching effects of different scavengers demonstrated that reactive h^+ and $O_2^{\bullet -}$ played the major role in the MO degradation. It was elucidated that the excellent photocatalytic activity of Ag_3PO_4/Ag/SiC for the degradation of MO under visible light (λ>420 nm) can be ascribed to the efficient separation of photogenerated electrons and holes through the Z-scheme system composed of Ag_3PO_4, Ag and SiC, in which the Ag nanoparticles acted as the charge transmission-bridge. The Ag_3PO_4/Ag/SiC hybrid remained good photocatalytic activity after 10 times of cycle experiments.

Introduction

Semiconductors-based photocatalysis is a promising environmental friendly strategy to solve the environmental contamination.[1, 2] Developing high-efficiency semiconductor photocatalysts is essential to transform this technology into practical applications. Unfortunately, most widely applied semiconductor photocatalysts are just active under UV-light irradiation, which greatly restricts their practical applications under solar light. Therefore, the development of high-efficiency visible-light-driven photocatalysts has become a hot topic in the photocatalysis field.

Recently, Ag-based photocatalysts, such as AgX (X=Cl, Br and I)[3-5], Ag_2O[6], Ag_2CO_3[7]and $Ag_6Si_2O_7$[8] have been developed for photocatalytic degradation of pollutants in wastewater. Among those Ag-based photo-catalysts, Ag_3PO_4 is extremely attractive since it has shown the remarkable quantum efficiency up to 90% in the O_2 evolution from photooxidation of water as well as photodecomposition of organic dye under visible light irradiation.[9] However, there are still some shortcomings inherent in Ag_3PO_4 photocatalytic systems[10]. As matter of fact, Ag_3PO_4 is slightly soluble in aqueous solution, which greatly hinders its application in the environmental management. Moreover, the by-product Ag particles usually generate from the photo-decomposition of Ag_3PO_4 in the absence of electron acceptor during the photocatalytic process, which would decrease its visible light absorption and photocatalytic activity. In order to enhance the photocatalytic activity and stability of Ag_3PO_4, several kinds of materials have cooperated with Ag_3PO_4 to generate hybrid photocatalysts and heterostructures. The combination of Ag_3PO_4 with carbon materials (oxidized graphene[11, 12], graphene[13, 14] and carbon quantum dots[15]) can prevent the recombination of photogenerated hole-electron pairs and accelerate the electron transportation because of the excellent electrical conductivity of carbon materials. However, the more negative conduction band potential of carbon materials greatly hinders the photogenerated electron transfer from Ag_3PO_4 to the carbon materials. Building heterostructures by cooperating Ag_3PO_4 with other semiconductors, which include wide-bandgap semiconductors (TiO_2, ZnO, SnO_2, et al)[16-20] and narrow-bandgap semiconductors ($BiMoO_4$, Cr-$SrTiO_3$, g-C_3N_4, et al)[21-25], is an valid route to facilitate the separation of photogenerated electron-hole pairs and thus enhance photocatalytic activity of Ag_3PO_4. But the obtained heterojunction structures suffer from the less reducibility and oxidability of the remaining electrons and holes.

More recently, with more and more attention has been paid to the mechanism of Ag_3PO_4-based hybrid photocatalytic systems, the by-product Ag has been found to be a charge transmission bridge in the Ag_3PO_4-based Z-scheme systems[26, 27]. It has been reported that the Ag_3PO_4-based Z-scheme systems can not only facilitate the charge separation but also retain the high reducibility and oxidability of the remaining electrons and holes for the corresponding photocatalysts. However, there are only few reports on the development of Ag_3PO_4-based Z-scheme system.[25,26]

In the current work, SiC, a semiconductor with a band gap of around 2.5 eV, was chosen to combine with Ag_3PO_4, and a novel high-efficiency Ag_3PO_4/Ag/SiC hybrid photocatalyst was demonstrated for the first time. The Ag_3PO_4/Ag/SiC hybrids with different mole ratios of SiC were synthesized via in-suit precipitation and were characterized by XRD, XPS, TEM and UV-vis spectrometer. The photocatalytic activities of the Ag_3PO_4/SiC hybrid

photocatalysts with different mole ratios of SiC were evaluated by degradation methyl orange (MO) under visible light (> 420 nm), and the optimal mole fraction of SiC in the hybrid was determined. Furthermore, the photocatalytic mechanism of the Ag_3PO_4/Ag/SiC hybrid photocatalyst was investigated via reactive species trapping experiments. It is shown that a Z-scheme system composed of Ag_3PO_4, Ag and SiC contributes to the enhanced photocatalytic activity of the hybrid. Finally, the stability of the Ag_3PO_4/Ag/SiC hybrid photocatalyst was examined.

Experiment Section

Preparation of Ag_3PO4/Ag/SiC photocatalysts

The Ag_3PO_4/Ag/SiC photocatalysts were synthesized by an in-situ precipitation method at room temperature. In a typical process, different amounts of SiC nanoparticles (Nanjing XFNANO Materials Tech Co., Ltd) were dispersed in 50 ml deionized water by ultrasound for 30 min, and then 50 ml 0.05M $AgNO_3$ aqueous solution was dropped into the SiC dispersed solution. After stirring for 30 min, 50 ml 0.075 M Na_2HPO_4 aqueous solution were added into the above solution drop by drop under magnetic stirring. After stirring for 1h, the suspension was irradiated by 300 W Xe lamp equipped with an optical cut-off filter (λ> 420 nm) for 15 min. Finally, the precipitate was washed with deionized water for 3 times and collected by centrifugation, and then dried at 60℃ in the vacuum drying oven. The obtained photocatalysts with different mole ratios of SiC were named as Ag_3PO_4/Ag/SiC-1%, Ag_3PO_4/Ag/SiC-5%,Ag_3PO_4/Ag/SiC-10%,andAg_3PO_4/Ag/SiC-20%, respectively. For comparison, Ag_3PO_4/Ag and SiC/Ag were also prepared.

For Ag_3PO_4/Ag, 50 ml 0.075 M Na_2HPO_4 aqueous solution were added into 50 ml 0.05M $AgNO_3$ aqueous solution drop by drop under magnetic stirring. After stirring for1h,the suspension was irradiated by 300 W Xe lamp equipped with an optical cut-off filter (λ> 420 nm) for 15 min. Finally, the precipitate was washed with deionized water for 3 times and collected by centrifugation, and then dried at 60℃ in the vacuum drying oven.

For SiC/Ag, the photo-reduced process was used, which is widely used in metallic Ag deposition[28-30]. SiC nanoparticles were dispersed in 50 ml deionized water by ultrasound for 30 min, and then were irradiated by 300 W Xe lamp equipped with an optical cut-off filter for 15 min. Finally, the precipitate was washed with deionized water for 3 times and collected by centrifugation, and then dried at 60℃ in the vacuum drying oven. Under visible light irradiation, the SiC excite and then the photogenerated electron will reduce the Ag^+ which absorb on the SiC surface in the $AgNO_3$ solution.

Characterization

The powder X-ray diffraction (XRD) measurements were performed on the D/max-ⅢA instrument using Cu Kα radiation at a scanning rate of 0.02 deg/s. Diffuse Reflectance Spectra (DRS)of the samples were obtained by a Shimadzu U-3010 spectrophotometer, equipped with an integrating sphere assembly. $BaSO_4$ was used as a reflectance standard. The morphologies of the samples were observed with a scanning electron microscope (S-3700N), and their energy-dispersive spectroscopy (EDS) was observed using an Oxford instruments

INCA 300 detector Transmission electron microscopy (TEM) images were obtained by using a JEM2100F field emission electron microscope. Photoluminescence(PL) spectra of the photocatalyst were recorded by using an F-4600 spectrometer with an excitation wavelength of 325nm. X-ray photoelectron spectroscopy (XPS) measurements were carried out on a THETA Prode spectrometer and the spectra were calibrated to the C 1s peak at 284.8 eV.

Evaluation of photocatalytic activity

The photocatalytic activities of the samples were evaluated by the degradation of MO and phenol aqueous solution with the concentration of 10 mg/L under UV-vis light irradiation. A 300W Xe lamp with a 420 nm cutoff filter was used as the light source. In each experiment, 0.1g of the as-prepared photocatalyst was added into 100 ml MO solution. Before irradiation, the suspensions containing the photocatalysts were stirred for 30 min in dark in order to reach the adsorption-desorption equilibrium. In the process of irradiation, a certain amount of the suspension was removed in every 5 min and centrifuged to obtain the clear solution. The absorbance of the clear solution was measured by a Shimadzu UV-2050 spectrophotometer.

In order to detecting the active species during the photocatalytic reaction, ammonium oxalate (AO), benzoquinone (BQ) and isopropanol (IPA) were added into the MO solution dispersed with the Ag_3PO_4/SiC hybrid photocatalyst to capture holes (h^+), the superoxide radicals ($O_2^{\bullet-}$) and hydroxyl radicals (•OH), respectively, followed by the photocatalytic activity test.

Results and Discussion

Fig.1 displays the XRD patterns of the Ag_3PO_4/Ag/SiC hybrid photocatalysts with different mole ratios of SiC, together with those of SiC/Ag and Ag_3PO_4/Ag. It is observed that no peaks assigned to Ag^o were found in the Ag_3PO_4/Ag/SiC, Ag_3PO_4/Ag and SiC/Ag owing to its low amount. Ag_3PO_4/Ag is cubic phase (JCPDS NO.06-0505), while SiC/Ag is a cubic crystal (JCPDS No. 65-0360). No obvious peaks of the SiC phases are found in the patterns of the Ag_3PO_4/Ag/SiC-1% because of the low contents and good dispersion of SiC. As the mole ratio of SiC is increased to 5%, 10% and 20%, the Ag_3PO_4/Ag/SiC hybrid photocatalysts exhibit a coexistence of both SiC and Ag_3PO_4 phases, and the intensities of the diffraction peaks of SiC increase with the weight ratio of SiC in the hybrids.

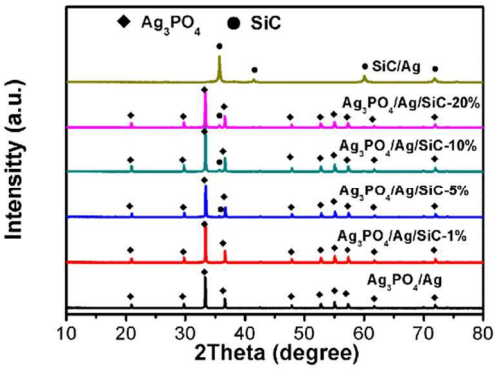

Fig. 1 XRD patterns of Ag_3PO_4/Ag, SiC/Ag and Ag_3PO_4/Ag/SiC hybrids with different mole ratios of SiC.

Fig. 2 displays the UV-vis diffuse reflectance spectra of the Ag_3PO_4/Ag/SiC hybrids with different mole ratios of SiC, together with those of Ag_3PO_4/Ag and SiC/Ag. As shown in Figure 2, SiC/Ag has an absorption edge at about 475 nm, while Ag_3PO_4/Ag has a

broader absorption in the visible region with an absorption edge at about 530 nm. The Ag_3PO_4/Ag/SiC samples show the similar absorption edge and a broader absorption in the visible region as comparison to Ag_3PO_4/Ag. According to the plot of $(ahv)^{2/n}$ versus energy, as shown in the insert of Figure 2, the band gap energies (Eg) of Ag_3PO_4 and SiC have been calculated to be 2.41 and 2.58 eV, respectively. The band structure of Ag_3PO_4 and SiC can be estimated according to the empirical equations 1 and 2 below;

$$E_{VB} = \chi - E^e + 0.5 * E_g \qquad (1)$$

$$E_{CB} = E_{VB} - E_g \qquad (2)$$

Where E_{VB} and E_{CB} is the valence and conduction band edge potential, respectively; χ is the electronegativity of the semiconductor, which is the geometric mean of the electronegativity of the constituent atoms; E^e is the energy of free electrons on the hydrogen-scale (about 4.5 eV vs. NHE). The χ values for SiC and Ag_3PO_4 are 5.46 and 6.16 eV, respectively. Thus, the E_{VB} of SiC and Ag_3PO_4 have been calculated to be 2.25 and 2.87 eV vs. NHE and their corresponding E_{CB} are –0.33 and 0.45 eV vs. NHE, respectively.

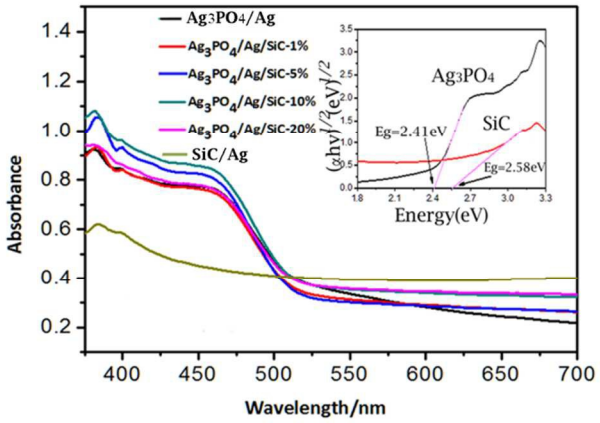

Fig. 2 UV-vis diffuses reflectance spectra of Ag_3PO_4/Ag, SiC/Ag, and Ag_3PO_4/Ag/SiC hybrids with different mole ratios of SiC (the insert shows plot of $(ahv)^{1/2}$ versus energy（hv）for Ag_3PO_4 and SiC).

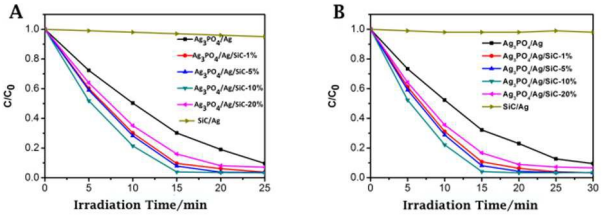

Fig. 3 Photocatalytic activity of Ag_3PO_4/Ag, SiC/Ag and Ag_3PO_4/Ag/SiC hybrids on degrading of MO (A) and phenol (B) under visible light irradiation

The photocatalytic activity of the as-prepared samples under visible light irradiation was also evaluated, as shown in Fig. 3. The photocatalytic degradation efficiency of these prepared samples follows the order Ag_3PO_4/Ag/SiC-10% > Ag_3PO_4/Ag/SiC-5% >Ag_3PO_4/Ag/SiC-1% > Ag_3PO_4/Ag/SiC-20% > Ag_3PO_4/Ag > SiC/Ag. This result clearly demonstrates that all the Ag_3PO_4/Ag/SiC hybrids exhibit higher photocatalytic activities than Ag_3PO_4/Ag and SiC/Ag, which suggests that combining Ag_3PO_4/Ag and SiC/Ag is an efficient route to enhance their photocatalytic activity. In the presence of Ag_3PO_4/Ag/SiC-10%, about 97% of the MO molecules were decomposed within 15 min under visible light. Furthermore, phenol, a substance without absorbing visible-light, was used to further verify the visible light photocatalytic activity of the as-prepared samples under visible light (> 420 nm), and the obtained results are illustrated in Figure 3B. All the Ag_3PO_4/Ag/SiC photocatalytic and pure Ag_3PO_4 exhibit excellent photocatalytic activities on degradation of phenol under visible light, confirming their inherent visible light photocatalytic properties. In addition, a comparison on the photocatalytic activity between Ag_3PO_4/Ag/SiC-10% and a mixture of SiC/Ag and Ag_3PO_4/Ag has been conducted, as shown in Fig.4. The mole ratios of SiC/Ag and Ag_3PO_4/Ag in the two samples are the same. It can be clearly seen from Fig.4 that the photocatalytic activity of Ag_3PO_4/Ag/SiC-10% is much higher than that of the mixture of SiC/Ag and Ag_3PO_4/Ag, implying that the efficient charge transmission and separation occurs in Ag_3PO_4/Ag/SiC-10% rather than in the mixture.

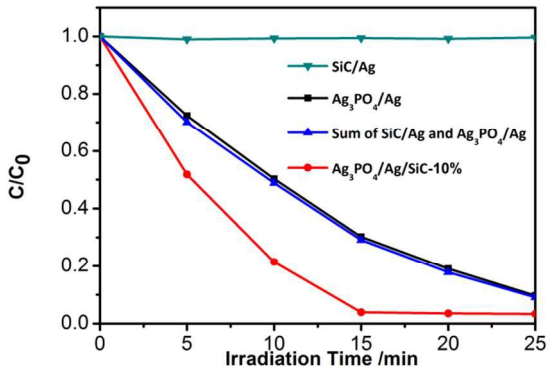

Fig.4 Comparison on the photocatalytic activity of Ag_3PO_4/Ag/SiC-10% with that of the mixture of Ag_3PO_4/Ag and SiC/Ag with the same weight fraction of SiC on the degradation of MO under visible light irradiation (> 420 nm).

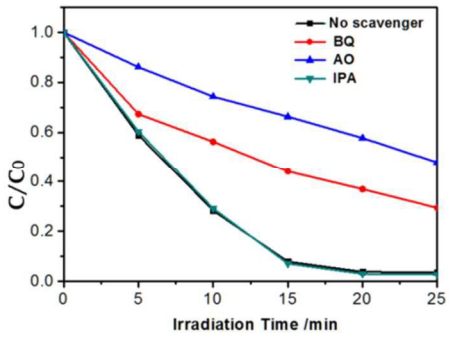

Fig.5 Photocatalytic activity of Ag_3PO_4/Ag/SiC-10%on the degradation MO in presence of different scavengers under visible light irradiation (> 420 nm).

To investigate the photocatalytic mechanism of the Ag_3PO_4/Ag/SiC-10% hybrid, the effect of scavengers on the degradation of MO was examined in the photocatalytic oxidation (PCO) process and the results are shown in Fig.5. Specifically,

ammonium oxalate (AO), benzoquinone (BQ) and isopropanol (IPA) acted as the scavengers for h^+, $O_2^{\bullet-}$ and •OH were introduced into the PCO process, respectively. As is clear from Figure 5, the addition of IPA did not affect the degradation rate of MO over Ag_3PO_4/Ag/SiC-10%, indicating that •OH was not the main reactive species in the photocatalytic process. In contrast, the photocatalytic degradation of MO was repressed in presence of AO and BQ. According to these results, it can be concluded that h^+ and $O_2^{\bullet-}$ are the main oxygen active species for Ag_3PO_4/Ag/SiC-10% in the MO solution under visible light irradiation. It can be inferred that the electrons left on the E_{CB} of SiC reduce O_2 to $O_2^{\bullet-}$ through one-electron reducing reaction because the E_{CB} potential of SiC is more negative than $E_0(O_2/O_2^{\bullet-})$ (–0.046 eV vs. NHE).

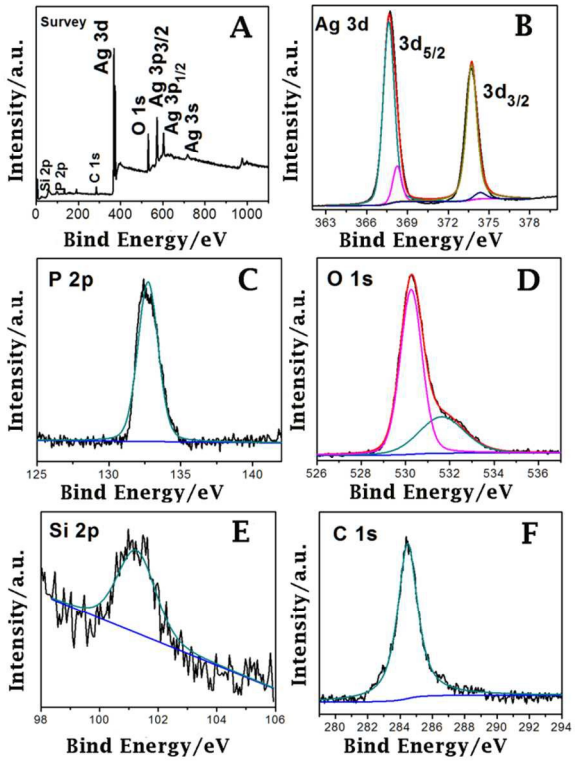

Fig.6 Survey (A), Ag 3d(B), P 2p (C), O 1s (D), Si 2p (E) and C 1s (F) XPS spectra of the fresh Ag_3PO_4/Ag/SiC-10% sample.

In order to confirm the existence of metallic Ag, XPS technology has been used to analyse the surface element composition and chemical state of Ag_3PO_4/Ag/SiC-10%, and the obtained results are shown in Fig.6. It is clearly seen that only Ag, P, O, Si and C elements were detected in the XPS survey spectrum (Fig.6A). As shown in Fig.6B, the Ag 3d peaks of Ag_3PO_4/Ag/SiC-10% has separated as Ag^+ peaks and Ag^0 peaks. The weak peaks at 368.13 and 374.22 eV are attributed to Ag^0 of Ag_3PO_4, indicating the existence of metallic Ag NPs on the surface of Ag_3PO_4/Ag/SiC-10% sample. The strong peaks at 367.5 and 373.4 eV are assigned to Ag^+ of Ag_3PO_4. A broad peak in the range of 131 to 135 eV of the P 2p spectrum (Fig. 6C) is observed for the Ag_3PO_4/Ag/SiC-10% sample which is corresponding to the phosphorus of Ag_3PO_4. The O 1s peak centered at 530.8 eV is associated with the O^{2-} in Ag_3PO_4. The other O 1s peak at 532.6 eV as a result of the presence of –OH group or a water molecule absorbed on the surface of theAg_3PO_4/Ag/SiC composite photocatalyst (Fig.6D). The peaks at 101.1 and 284.8 eV can be attributed to Si 2p and C 1s of SiC (Fig.6E and 6F). Moreover, the metallic Ag content on the surface of the as-prepared samples calculated from XPS results are listed in Table1. It can be clearly found that the metallic Ag content on the surface of each sample is about 12% in atom, suggesting that controlling the irradiation time can efficiently control the metallic Ag content.

Table 1 Metallic Ag content in each sample from XPS and EDS

CATALYST	Metallic Ag Atom Content (at %)	
	From XPS	From EDS
Ag_3PO_4/Ag	12.46	7.23
Ag_3PO_4/Ag/SiC-1%	12.27	7.19
Ag_3PO_4/Ag/SiC-5%	12.44	7.21
Ag_3PO_4/Ag/SiC-10%	12.34	7.15
Ag_3PO_4/Ag/SiC-20%	12.28	6.96
SiC/Ag	12.71	7.33

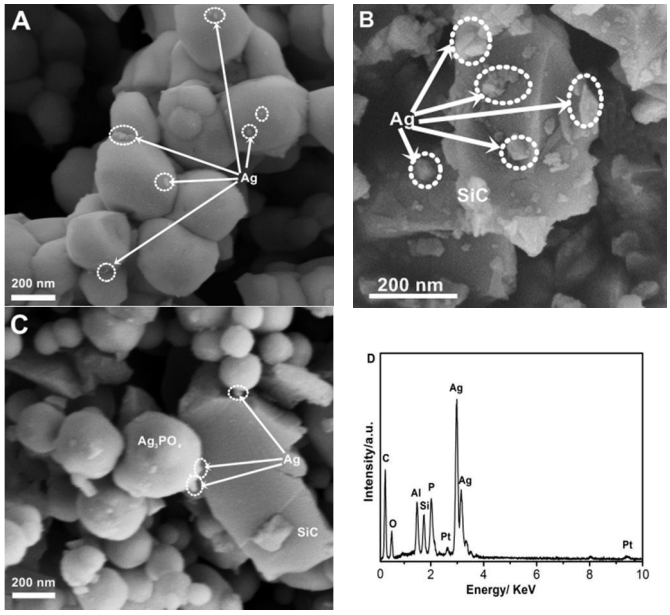

Fig. 7 SEM images of Ag_3PO_4/Ag(A), SiC/Ag(B) and Ag_3PO_4/Ag/SiC-10% (C), together with the EDS spectrum of Ag_3PO_4/Ag/SiC-10% (D).

The SEM images of Ag_3PO_4/Ag, SiC/Ag and Ag_3PO_4/Ag/SiC-10% together with EDS spectrum are shown in the Fig.7. The as-prepared Ag_3PO_4/Ag particles are irregular Ag_3PO_4 sphere about 150-250 nm with some small Ag nanoparticles about 10 nm on its surface. The SiC particles are irregular polyhedron about 500 nm with Ag aggregation about 30 nm on its surface. In the Fig.7C, Ag_3PO_4 nanoparticles about 150-200 nm randomly covered on the surface of SiC particles. Moreover, it can be clearly found that the metallic Ag about 10 nm size existed on the junction of Ag_3PO_4 and SiC. It can be clearly found that all the peaks are corresponding to the elemental composition of SiC, Ag and Ag_3PO_4 in the EDS spectrum, as shown in Fig. 7D. Furthermore, the metallic Ag content in the as-prepared samples calculated from EDS are listed in Table 1. The metallic Ag in each sample is about 7% in atom and vibrated in a negligible range, suggesting that controlling the irradiation time can efficiently control the metallic Ag content too. The metallic Ag content calculated from EDS is lower than that calculated from XPS is due to the XPS just can detect the surface elements and the metallic Ag only exist on the surface of the as-prepared sample.

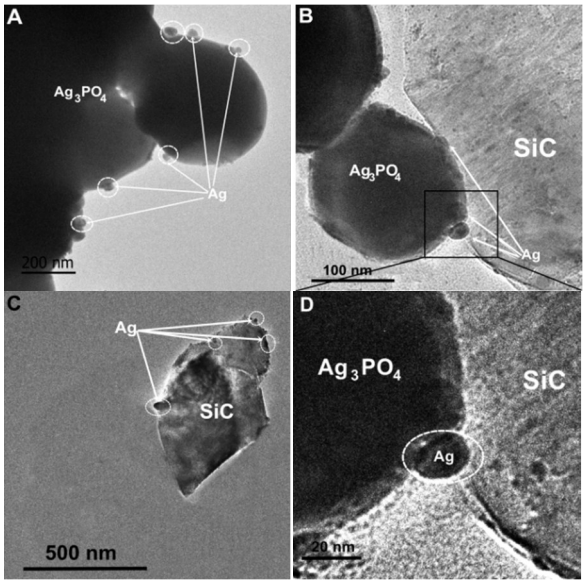

Fig. 8 TEM images of Ag_3PO_4/Ag (A), Ag_3PO_4/Ag/SiC-10% (B and D) and SiC/Ag (C).

Moreover, the component and connection of Ag_3PO_4/Ag, Ag_3PO_4/Ag/SiC-10% and SiC/Ag were investigated by TEM, as shown in Fig.8. It can be clearly found that the metallic Ag is form on the surface of Ag_3PO_4 and SiC. For the Ag_3PO_4/Ag/SiC-10% photocatalyst, Ag_3PO_4 particles with the size about 200 nm were well anchored on the surface of SiC, and the metallic Ag NPs with the size about 10 nm on the junction of Ag_3PO_4 and SiC, which is well agree with the SEM results. According to the SEM and TEM results, the metallic Ag nanoparticles in the Ag_3PO_4/Ag/SiC hybrid photocatalyst is formed on the junction of $Ag_3PO_4$and SiC, which can act as a charge transmission bridge in the hybrid catalyst.

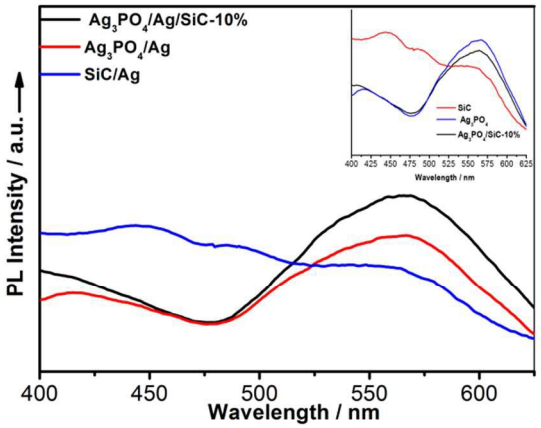

Fig.9 PL spectra of Ag_3PO_4/Ag, Ag_3PO_4/Ag/SiC-10% and SiC/Ag, (inset is the PL spectra of Ag_3PO_4, SiC and Ag_3PO_4/SiC-10%) with an excitation wavelength of 325 nm.

The photoluminescence (PL) emission spectra were conducted to investigate the charge recombination and transfer behaviour of the Ag_3PO_4/Ag/SiC photocatalyst and the results were shown in Fig. 9. It is well-known that there combination of electron–hole pairs can release energy in the form of PL emission. In general, a lower PL intensity indicates lower recombination of charge carriers, leading to higher photocatalytic activity[27]. However, the Ag_3PO_4/Ag/SiC-10% with the higher photocatalytic activity showed a higher PL intensity than that of Ag_3PO_4/Ag and SiC/Ag. The higher PL intensity of Ag_3PO_4/Ag/SiC-10% would be attributed to higher recombination of photogenerated electron-hole pairs in the metallic Ag. This is because the metallic Ag formed on the surface of Ag_3PO_4 and SiC process suitable wave function[26, 31, 32], the photogenerated electron in the CB of Ag_3PO_4 and holes in the VB of SiC will shift to the metallic Ag simultaneously and then combine here, which lead to higher PL intensity. The recombination in the metallic Ag is favourable for accelerating the separation of the photogenerated electron-hole pairs in both Ag_3PO_4 and SiC, so the photocatalytic performance of Ag_3PO_4/Ag/SiC improved. Moreover, it can be clearly seen that the PL intensities of Ag_3PO_4/SiC-10% hybrid photocatalysts were lower than that of Ag_3PO_4 and SiC because of the formation of heterojunction between Ag_3PO_4 and SiC can efficiently suppress the recombination of the photogenerated electron–hole in the Ag_3PO_4/SiC-10% hybrid photocatalysts. On the basis of these results, it concluded that the Ag_3PO_4/Ag/SiC system is a typical Z-scheme photocatalyst rather than heterojunction photocatalyst. It is suggested that rich electrons in the CB of SiC and holes in the VB of Ag_3PO_4 participate in the reduction reaction of dissolved O_2 and the oxidation of MO, respectively.

According to the above results, the possible photocatalytic mechanism of the Ag_3PO_4/Ag/SiC hybrid photocatalyst is shown in Scheme. 1. The PO_4^{3-} ions with large negative charge in Ag_3PO_4 prefer to repel electrons and attract holes, which is in favour of the formation visible-light-driven Ag_3PO_4/Ag/SiC Z-scheme system. And the Ag NPs act as the charge transmission-bridge to form the visible-light-driven Ag_3PO_4/Ag/SiC Z-scheme system. Under visible light irradiation, both Ag_3PO_4 and SiC are excited, and the photogenerated holes and electrons are in their conduction and valence band, respectively. The electrons on the conduction band minimum (CBM) of Ag_3PO_4 easily shift into metal Ag (electron transfer I: Ag_3PO_4 CBM→Ag) through the Schottky barrier because the CB potential of Ag_3PO_4 is more negative than that Fermi level of the loaded metal Ag. Meanwhile，the holes on the valence band maximum (VBM) VBM of SiC also easily shift into metal Ag (hole transfer II: SiC VBM→Ag) because the Fermi level of Ag is more positive than the VBM of SiC, and then combine with the electron here. Therefore, simultaneous electron (I) and hole (II) transfers enhance the charge separation of Ag_3PO_4 and SiC. And holes in the E_{VB} of Ag_3PO_4 show strong oxidation ability while the electrons in the E_{CB} of SiC with more negative potential display strong reduction power.

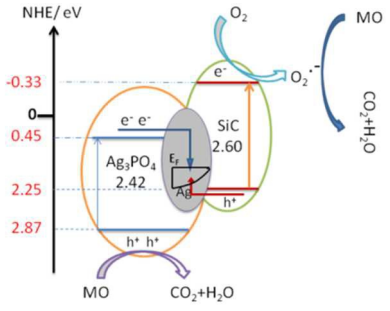

Scheme. 1 Schematic illustration of photocatalytic mechanism of Ag_3PO_4/Ag/SiC under visible light irradiation (>420 nm).

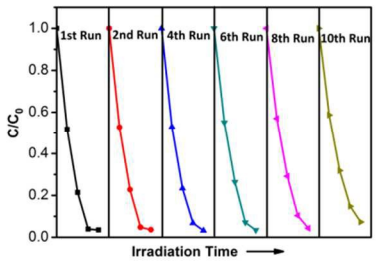

Fig.10 Cycle runs of Ag_3PO_4/Ag/SiC -10% for degradation of MO under visible light irradiation (> 420 nm).

The stability and reusability of Ag_3PO_4/Ag/SiC photocatalysts were evaluated by the cycling degradation experiment and the results are shown in Fig.10. The results show that the Ag_3PO_4/Ag/SiC photocatalysts do not display obvious decrease of photocatalytic degradation activity under visible light, indicating that the Ag_3PO_4/Ag/SiC hybrid photocatalysts is sufficient stable for photocatalytic degradation of MO. The extraordinary stability of Ag_3PO_4/Ag/SiC photocatalysts is ascribed to the fast charge separation of Ag_3PO_4/Ag/SiC induced by Z-scheme system. For pure Ag_3PO_4, the photogenerated electrons are prone to remain on the Ag_3PO_4 and then degraded the Ag_3PO_4 to generate the by-product metallic Ag. For theAg_3PO_4/Ag/SiC-10% photocatalyst, the photogenerated electrons are apt to migrate to the metallic Ag and combine with the hole here, which can efficient suppress the self-degradation of Ag_3PO_4 induced by photogenerated electron. Moreover, the crystalline structure and morphology of Ag_3PO_4/Ag/SiC-10% photocatalyst after photocatalytic experiments have been investigated by XRD and SEM. There is no evident crystalline structure or morphology changes could be observed in either their XRD patterns or SEM results, indicating that these Ag_3PO_4/Ag/SiC photocatalysts possess high stability.

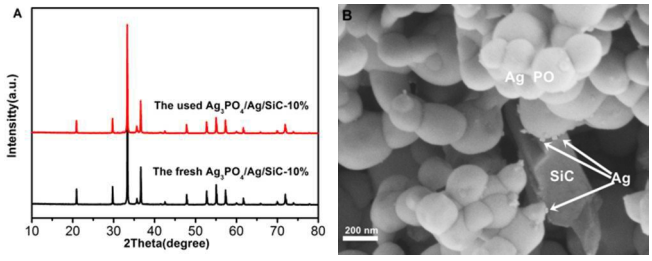

Fig.11 XRD patterns and SEM images of the Ag_3PO_4/Ag/SiC-10% after photocatalytic experiments.

Conclusions

Novel high-efficiency visible-light-driven Ag_3PO_4/Ag/SiC Z-systems have been successfully prepared via facile in-suit precipitation process under room condition. The Ag_3PO_4/Ag/SiC photocatalysts showed obviously superior photocatalytic activity over that of Ag_3PO_4/Ag and SiC/Ag for the photo-degradation of MO and phenol under visible light irradiation. The superior photocatalytic activity of Ag_3PO_4/Ag/SiC may originate from the efficient separation of photogenerated electron-hole pairs through the Z-scheme system composed of Ag_3PO_4, Ag and SiC. The Z-scheme photocatalytic process of the hybrid photocatalysts was also supported by active species trapping and PL experiment results. Furthermore, Ag_3PO_4/Ag/SiC possessed good stability in the PCO process under visible light irradiation. It is expected that the Ag_3PO_4/Ag/SiC with high photocatalytic activities will greatly promote their practical application to eliminate organic pollutants.

Acknowledgements

This work was supported by the National Natural Science Foundation of China (No.21276088 and 60976053)

Notes and references

Key Laboratory of Enhanced Heat Transfer and Energy Conservation, the Ministry of Education, School of Chemistry and Chemical Engineering, South China University of Technology, Guangzhou 510640, China
Corresponding author Tel:86-20-87112997; Fax: 86-20-87113870.
E-mail address: cexmfang@scut.edu.cn.

† Electronic Supplementary Information (ESI) available: [details of any supplementary information available should be included here]. See DOI: 10.1039/b000000x/

1. X. L. Hu, G. S. Li and J. C. Yu, *Langmuir*, 2010, **26**, 3031-3039.
2. A. Kubacka, M. Fernández-García and G. Colón, *Chem. Rev.*, 2011, **112**, 1555-1614.
3. P. Wang, B. B. Huang, X. Y. Qin, X. Y. Zhang, Y. Dai, J. Y. Wei and M. H. Whangbo, *Angew. Chem.-Int. Edit.*, 2008, **47**, 7931-7933.
4. P. Wang, B. B. Huang, X. Y. Zhang, X. Y. Qin, H. Jin, Y. Dai, Z. Y. Wang, J. Y. Wei, J. Zhan, S. Y. Wang, J. P. Wang and M. H. Whangbo, *Chem.-Eur. J.*, 2009, **15**, 1821-1824.
5. C. Hu, T. W. Peng, X. X. Hu, Y. L. Nie, X. F. Zhou, J. H. Qu and H. He, *J. Am. Chem. Soc.*, 2010, **132**, 857-862.
6. X. F. Wang, S. F. Li, H. G. Yu, J. G. Yu and S. W. Liu, *Chem.-Eur. J.*, 2011, **17**, 7777-7780.
7. C. W. Xu, Y. Y. Liu, B. B. Huang, H. Li, X. Y. Qin, X. Y. Zhang and Y. Dai, *Appl. Surf. Sci.*, 2011, **257**, 8732-8736.
8. Z. Lou, B. Huang, Z. Wang, X. Ma, R. Zhang, X. Zhang, X. Qin, Y. Dai and M.-H. Whangbo, *Chem. Mat.*, 2014, **26**, 3873-3875.
9. Z. G. Yi, J. H. Ye, N. Kikugawa, T. Kako, S. X. Ouyang, H. Stuart-Williams, H. Yang, J. Y. Cao, W. J. Luo, Z. S. Li, Y. Liu and R. L. Withers, *Nat. Mater.*, 2010, **9**, 559-564.
10. Y. Bi, S. Ouyang, J. Cao and J. Ye, *Physical Chemistry Chemical Physics*, 2011, **13**, 10071-10075.
11. Y. Ao, P. Wang, C. Wang, J. Hou and J. Qian, *Appl. Surf. Sci.*, 2013, **271**, 265-270.
12. H. Cui, X. Yang, Q. Gao, H. Liu, Y. Li, H. Tang, R. Zhang, J. Qin and X. Yan, *Mater. Lett.*, 2013, **93**, 28-31.
13. P. Dong, Y. Wang, B. Cao, S. Xin, L. Guo, J. Zhang and F. Li, *Applied Catalysis B-Environmental*, 2013, **132**, 45-53.
14. X. F. Yang, H. Y. Cui, Y. Li, J. L. Qin, R. X. Zhang and H. Tang, *ACS Catal.*, 2013, **3**, 363-369.
15. H. Zhang, H. Huang, H. Ming, H. Li, L. Zhang, Y. Liu and Z. Kang, *J. Mater. Chem.*, 2012, **22**, 10501-10506.
16. W. Yao, B. Zhang, C. Huang, C. Ma, X. Song and Q. Xu, *J. Mater. Chem.*, 2012, **22**, 4050-4055.
17. X. Ma, H. Li, Y. Wang, H. Li, B. Liu, S. Yin and T. Sato, *Appl. Catal. B-Environ.*, 2014, **158**, 314-320.

18. W. Liu, M. Wang, C. Xu, S. Chen and X. Fu, *Mater. Res. Bull.*, 2013, **48**, 106-113.
19. L. Zhang, H. Zhang, H. Huang, Y. Liu and Z. Kang, *New J. Chem.*, 2012, **36**, 1541-1544.
20. B. Cao, P. Dong, S. Cao and Y. Wang, *J. Am. Ceram. Soc.*, 2013, **96**, 544-548.
21. G. Fu, G. Xu, S. Chen, L. Lei and M. Zhang, *Catal. Commun.*, 2013, **40**, 120-124.
22. J. Guo, S. Ouyang, P. Li, Y. Zhang, T. Kako and J. Ye, *Appl. Catal. B-Environ.*, 2013, **134**, 286-292.
23. S. Kumar, T. Surendar, A. Baruah and V. Shanker, *J. Mater. Chem. A*, 2013, **1**, 5333-5340.
24. C. J. Li, P. Zhang, R. Lv, J. W. Lu, T. Wang, S. P. Wang, H. F. Wang and J. L. Gong, *Small*, 2013, **9**, 3951-3956.
25. H. Yu, Z. Jiao, H. Hu, G. Lu, J. Ye and Y. Bi, *CrystEngComm*, 2013, **15**, 4802-4805.
26. Z. Chen, W. Wang, Z. Zhang and X. Fang, *The Journal of Physical Chemistry C*, 2013, **117**, 19346-19352.
27. H. Katsumata, T. Sakai, T. Suzuki and S. Kaneco, *Ind. Eng. Chem. Res.*, 2014, **53**, 8018-8025.
28. P. A. Gross, S. N. Pronkin, T. Cottineau, N. Keller, V. Keller and E. R. Savinova, *Catal. Today*, 2012, **189**, 93-100.
29. B. Divband, M. Khatamian, G. R. K. Eslamian and M. Darbandi, *Appl. Surf. Sci.*, 2013, **284**, 80-86.
30. W. Jiang, H. Z. Liu, L. Yin and Y. C. Ding, *J. Mater. Chem. A*, 2013, **1**, 6433-6440.
31. H. L. Lin, J. Cao, B. D. Luo, B. Y. Xu and S. F. Chen, *Catal. Commun.*, 2012, **21**, 91-95.
32. L. Q. Ye, J. Y. Liu, C. Q. Gong, L. H. Tian, T. Y. Peng and L. Zan, *ACS Catal.*, 2012, **2**, 1677-1683.

Novel Z-Scheme Visible-Light-Driven Ag_3PO_4/Ag/SiC photocatalysts with Enhanced Photocatalytic Activity

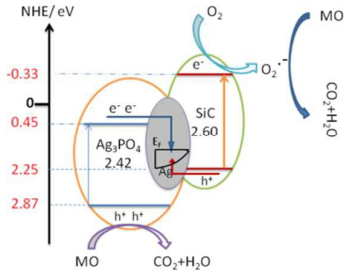

The excellent photocatalytic activity of Ag_3PO_4/Ag/SiC can be ascribed to the efficient separation of photogenerated electron-hole pairs through the Z-scheme.